J. Phys. Chem. A **1998,** *102,* 6513−6524 **6513**

Triplet State *Z*/*E*-Photoisomerizations of Polyenes: A Comparison of ab Initio and Density Functional Methods

Maria Brink, Helene Jonson, and Carl-Henrik Ottosson*,†

Department of Organic Chemistry, Chalmers University of Technology, S-412 96 Göteborg, Sweden

Received: October 17, 1997; In Final Form: May 18, 1998

In the search for less CPU-costly methods for study of triplet state *Z*/*E*-photoisomerization of olefins, Kohn−Sham density functional theory (DFT) has been tested on 1,3-butadiene (**BD**) and 1,3,5-hexatriene (**HT**). Computed T_1 energies were compared to those from CASSCF, CASPT2, and spin-projected UMP4(SDTQ) calculations as well as experiments. For both molecules it is necessary that nonlocal gradient corrections are made to the exchange functional since usage of the local spindensity approximation for exchange in most cases leads to vertical and relaxed T_1 energies that are too high. Gradient-corrected DFT as well as hybrid functional methods lead to T_1 energies that are bracketed by the corresponding UMP4(SDTQ) and CASPT2 energies and lie at most 4 kcal/mol below measured values. The relaxed T_1 energies for planar geometries are in slightly better agreement with experiment when calculated by pure nonlocal gradient-corrected DFT than by hybrid functional methods. However, T_1-state potential energy surfaces obtained by either type of method explain the experimental observations on triplet-state *Z*/*E*-photoisomerizations of **BD** and **HT**, and geometries of T_1 isomers of **BD** and **HT** compare well with those from UMP4(SDQ), UMP2, and CASSCF calculations. Finally, it should be noted that for both molecules UHF deviates from the higher computational levels in T_1 energies by 20−30 kcal/mol and should be avoided in all computations of T_1 states of olefins.

Introduction

Photorearrangements of olefins are important processes within both chemistry and biology. For instance, substituted polyenes are the light-absorbing units of the retinal proteins in the visual pigments as well as in 7-dehydrocholesterol, which is converted photochemically into previtamin-D3.[1] The rearrangements can take place in excited singlet or triplet states, and often, the outcome of the photochemistry is different in the two states. One important type of olefin photorearrangements is *Z*/*E*-isomerizations,[2] and throughout the last decades there has been an effort to clarify the underlying mechanisms of these processes. It is now accepted that they occur by either of two different mechanisms, namely, the adiabatic and diabatic, and central to which mechanism is followed is the shape of the potential energy surface (PES), as shown in Scheme 1.[3] In an adiabatic process the product is formed in an excited state from where decay to the ground state takes place (I), whereas in a diabatic process the decay occurs at an intermediate perpendicular geometry (II).

In the field of computational chemistry, the versatility of quantum chemical methods based on Kohn−Sham density functional theory (DFT) has been revealed,[4] also in the study of open-shell species. It has been shown by Cramer and coworkers that singlet−triplet energy gaps for a variety of systems, when compared to high-level ab initio calculations such as multireference configuration interaction (MRCI), are well described with nonlocal gradient-corrected DFT methods.[5−10] Bérces and Zgierski found that the geometry, energy, and frequencies of the first triplet excited state of the computationally challenging difluorosilylene were satisfactorily described with standard DFT methods based on Kohn−Sham theory.[11] However, when higher excited states of SiF_2 were computed, the deviations were large, showing that DFT methods are only applicable to the ground state and the lowest state of each symmetry. It should be noted that the Hohenberg−Kohn theorem indeed is valid for the lowest electronic state of each irreproducible representation.[12,13] Accordingly, methods based on Kohn−Sham theory, and thereby on the Hohenberg−Kohn theorem, are possible to apply when calculating open-shell species under the condition that the electronic states are the lowest of each specific symmetry.

SCHEME 1

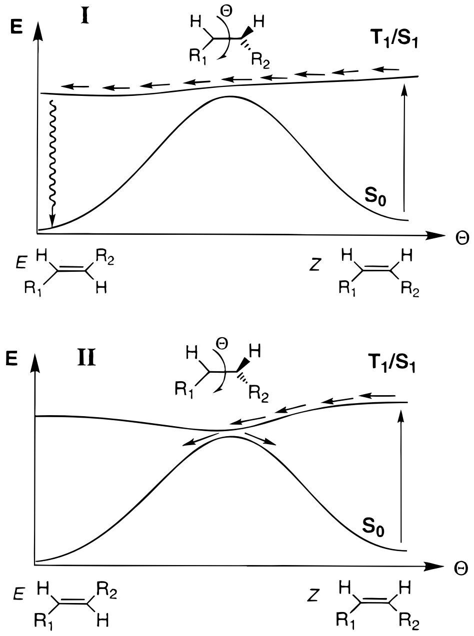

[†] Present address: Department of Chemistry and Biochemistry, University of Colorado, Boulder, CO 80309-0215.

S1089-5639(97)03384-7 CCC: $15.00

An attractive feature of DFT methods is the low spin contamination that normally results when calculating open shell species, contrary to UHF.[14] Indeed, if one could derive the exact density functionals for the Schrödinger Hamiltonian, it would be possible to perform calculations without spin contamination. This stems from the fact that the exact wave functions are eigenfunctions of $\hat{S}^2$. However, DFT methods based on the approximate density functionals that must be used are affected to a small extent by spin contamination, but not to the same extent as UHF.[14]

To our knowledge, there is no study that reveals how DFT methods work to describe the complete potential energy surface of a photochemical triplet-state reaction. Since there are no restrictions from theory to calculate both the S_0 and T_1 PES for *Z*/*E*-isomerization reactions of olefins with DFT methods, this is a pending issue that needs to be resolved. If one can show that a correctly chosen DFT method gives a good description of the T_1 PES for *Z*/*E*-isomerizations of small polyenes, then one could extend the study to larger systems. This should be of major interest since DFT methods are computationally cheap compared to conventional high level ab initio methods but lead to results that are of comparable or even better quality than second-order Møller−Plesset perturbation theory. To make a verdict about the utility of various DFT methods to calculate T_1 PES for olefin Z/*E*-isomerizations, they should be compared to calculations with well-established ab initio methods on shorter polyenes.

Hybrid functionals have often been shown to give slightly better results than pure DFT methods. However, for open-shell species such methods could give dubious results since they contain a HF kernel which might lead to higher spin contamination or affect the result in another way. Worth noting is that, it has been argued that spin projection is not suitable with DFT methods. For instance, Pople, Gill, and Handy wrote that "a KS determinant (for a radical or a triplet), which is *not* spin-contaminated, is *wrong*".[15] This fact was recently demonstrated by Wittbrodt and Schlegel, since they found that spin projection of unrestricted DFT energies gave less good results for homolytic dissociations than the unprojected energies.[16] On the other side, Houk and co-workers reported results for the Diels−Alder reaction that partially contradicted this fact.[17] The spin-correction procedure overcorrects for triplet contamination, but allows the energies for the diradical reaction pathway to be determined. In addition, Edgecombe and Becke showed that spin projection of B3P86 energies according to an approximate formula gave results that are in better agreement with experiments and high-level ab initio calculations than unprojected methods for the distance and dissociation energy of Cr_2.[18] However, since we found that spin contamination of T_1 states of olefins calculated by DFT is low, we kept to the unprojected formalism throughout this study.

We now report comparative calculations on 1,3-butadiene and 1,3,5-hexatriene where in the latter case we consider isomerization around both central and terminal CC double bonds. Through the possible combinations of local or nonlocal exchange functionals with local or nonlocal correlation functionals one can obtain an understanding of what effects are most important for a proper description of polyene T_1 states and the singlet−triplet energy splitting (ΔE_{S-T}). With regard to exchange functionals, either the local spin-density functional of Slater (S)[19] or the nonlocal gradient-corrected functional of Becke (Becke88 or simply B)[20] was utilized. The correlation functionals used were the local spin-density correlation functional of Vosko−Wilk−Nusair (VWN)[21] or the nonlocal gradient-corrected correlation functionals of either Lee−Yang−Parr (LYP)[22] or Perdew−Wang (PW91).[23] Thus, the combinations investigated were SVWN, SLYP, BVWN, BLYP, and BPW91. Finally, usage of hybrid functionals was tested with the three-parameter formula of Becke (B3)[24] in combinations B3LYP and B3PW91. Results from the DFT calculations were compared with results from CASSCF, CASPT2, and spin-projected UMP4(SDTQ) calculations, as well as experiments.

For 1,3-butadiene (**BD**) the vertical $S_0 \rightarrow T_1$ excitation has been determined experimentally at 3.22 eV (74.2 kcal/mol)[25] and within the range 3.14−3.60 eV (72.2−82.8 kcal/mol)[26−31] when using high-quality ab initio quantum chemical methods. From the first feature of the $S_0 \rightarrow T_1$ absorption spectrum the relaxed T_1 energy of **BD** was found to be 59.7 kcal/mol.[32] From quantum chemical calculations it was found that the C_s-symmetric structure with a C═C bond twisted 90° is 2.8−11.2 kcal/mol below the planar C_{2h}-symmetric structure.[33−39] Among the better of these studies is the MCSCF study by Aoyagi et al., where an energy difference of 3.2 kcal/mol was found.[37] This is in acceptable accordance with experiments by Wilbrandt, Orlandi, and co-workers which indicate that the twisted form of **BD** in the T_1 state is at most 2 kcal/mol below the planar form.[40]

With regard to 1,3,5-hexatriene (**HT**) it was found that twisting around the central C═C bond is responsible for the decay to S_0 from the T_1 PES.[41−43] The vertical excitation energies for $S_0 \rightarrow T_1$ are 59.4 and 60.8 kcal/mol for *E*-**HT** and *Z*-**HT**, and the 0−0 energy gaps, derived from the first feature of the $S_0 \rightarrow T_1$ absorption spectra, are 46.9 and 47.7 kcal/mol, respectively.[44] However, the uncertainty with regard to the 0−0 gaps is at least 0.5 kcal/mol. Furthermore, in both **HT** and 2,5-dimethyl-1,3,5-hexatriene the minima at *E* and twisted geometries are roughly isoenergetic (within 1 kcal/mol), and these minima are separated by a barrier sufficiently low to allow equilibration during the T_1 lifetime.[45] Thus, the PES for twisting around the central double bond in **HT** should be rather flat.

Information about rotation of a terminal C═C bond in **HT** can be obtained from 1,2-divinylcyclopentene (**DVCP**), which is a configurationally locked *Z*-**HT**.[46] The activation energy for triplet decay in this molecule was found to be 2.0 kcal/mol, i.e., larger than in *Z*-**HT**, where it is 0.7 kcal/mol. Since DVCP is locked around the central C═C bond, this could be the energy needed to twist around one of the terminal C═C bonds in the **HT** unit. However, it could also be the energy needed to distort the central C═C bond in **DVCP** so that a geometry is reached where spin−orbit coupling is sizable and the T_1-S_0 gap is sufficiently small so that decay to S_0 can occur.

From computations it has been found that *Z*/*E*-isomerization of the central C═C bond in **HT** indeed is easier than isomerization of a terminal C═C bond. The most recent study was made by Kikuchi and coworkers at the UHF/STO-3G level.[47,48] Calculations at more sophisticated levels of theory were performed by Orlandi and co-workers.[49] At the CASSCF(6,6)/6-31G(d,p) level the vertical $S_0 \rightarrow T_1$ excitation is well described, whereas ROHF gives a value that deviates by 9.0 kcal/mol from experiment. It was found at the CASSCF level that the *Z*-isomer is 2.4 kcal/mol less stable than the *E*-isomer. Moreover, the conformation with the central C═C bond rotated ~90° lies 0.4 kcal/mol below the *E*-isomer, and the barrier that separates twisted and *E*-isomers is approximately 1 kcal/mol. Finally, Malrieu and co-workers used the nonempirical Heisenberg Hamiltonian and found an energy lowering of 1.9 kcal/mol for twist around the central C═C bond and a barrier of 3.6 kcal/mol for rotation of a terminal C═C bond.[36]

A note should be given to the difference in triplet- and singlet-state photochemistry of the two polyenes. A variety of products are formed upon excitation to the singlet surfaces,[50,51] and crucial for the singlet photochemistry are conical intersections where excited- and ground-state surfaces meet to become degenerate.[52] Important features of conical intersections are that a fully efficient decay to the ground state within less than one vibrational period can occur and that they provide access to a number of ground-state pathways leading to different photoproducts. However, conical intersections take place between states of the same multiplicity, and the absence of such intersections between T_1 and S_0 states is a factor that leads to a different photochemistry of polyenes in T_1 and S_1 states. Decay from T_1 states instead occurs by intersystem crossing, which for an olefin is governed mainly by spin−orbit coupling.

For **BD**, the one-photon excitation takes the molecule to the 1^1B_u state. However, internal conversion from the 1^1B_u to the 2^1A_g state occurs, and the photochemistry continues in the latter state. In this state a conical intersection region between the ground state 1^1A_g and the singlet excited state 2^1A_g is easily reached,[53] and the photochemical reactions that can occur by passage through this intersection range from *s-cis/s-trans* and *Z*/*E*-isomerization to cyclobutene and bicyclobutane formation. Also for **HT**, similar conical intersection regions can be reached when in the 2^1A_g state.[54] One of these regions is responsible for the *Z*/*E*-isomerization and is reached after overcoming a small barrier of 6 kcal/mol as calculated at the CASSCF/cc-pVDZ level.

Thus, there are differences in the singlet- and triplet-state photochemistry of **BD** and **HT**, and which regions of the excited T_1 and S_1 surfaces are possible to reach is governed by their shapes. A good description of the T_1 PES is therefore necessary in order to get more knowledge on for instance the underlying rules behind diabatic and adiabatic *Z*/*E*-photoisomerizations. Accordingly, we decided to undertake an investigation on how computationally cheap DFT methods perform in calculations of T_1 PESs for such rearrangements. The main objective was to find out which method gives the best agreement with experiment as well as high-quality ab initio methods, and we hope that this should better enable future investigations of T_1-state *Z*/*E*-isomerizations of larger olefins.

Computational Methods

Initial calculations of the possible conformers of **BD** and **HT** in S_0 and T_1 states were performed at restricted and unrestricted HF, BVWN, BLYP, and B3LYP levels using the 3-21G basis set of Pople and co-workers.[55] Calculations were improved by using the 6-3lG(d,p) valence double-zeta basis set of Pople and Hariharan.[56] Frequencies were calculated with these methods using the 6-31G(d,p) basis set in order to verify if calculated stationary points correspond to minima or transition states.

The investigation of **BD** and **HT** with electron-correlated ab initio methods was started with Møller−Plesset second-order perturbation theory (MP2), using the 6-31G(d,p) basis set with all electrons included in the correlation treatment. Computations were improved by usage of the correlation consistent cc-pVDZ basis set of Dunning.[57] To check on the quality of the UMP2-(full)/cc-pVDZ triplet-state geometries, UMP4(SDQ,full)/cc-pVDZ geometry optimizations were performed at the planar and twisted geometries for the T_1 state of **BD**. Single-point UMP4-(SDTQ)/cc-pVDZ calculations were done at fully optimized UMP2(full)/cc-pVDZ geometries, as well as on geometries where C−C═C−H or C−C═C−C dihedral angles were frozen consecutively at 10°, 30°, 60°, 80°, 100°, 120°, 150°, and 170°, while all other geometry parameters were optimized. For **BD** all electrons were correlated at UMP4(SDTQ), whereas for **HT** the frozen core approximation was used. UMP4(SDTQ) energies for open-shell species were spin-projected by annihilation of unwanted spin states.[58]

In the CASSCF calculations, the active spaces were chosen so as to include all valence orbitals of π-character. This implies for **BD** that four electrons were placed into four orbitals (CASSCF(4,4)) and for **HT** that six electrons were placed into six active orbitals (CASSCF(6,6)). The number of reference determinants for **BD** are 20 for the S_0 state and 15 for the T_1 state, whereas for **HT** these states are described by 175 and 189 determinants, respectively. The 6-31G(d,p) basis set was utilized in the CASSCF geometry optimizations. To improve the CASSCF calculations, multiconfigurational SCF calculations with second-order perturbation theory (CASPT2)[59] was applied. These CASPT2 calculations were based on optimal CASSCF/6-31G(d,p) geometries and were performed with the atomic natural orbital basis set (14s9p4d/8s4p) of Roos and co-workers (ANO-L) in the contraction [6s3pld/2slp].[60] The second-order perturbation treatment in the CASPT2 calculations used CASSCF wave functions as reference wave functions in which all π-orbitals were included in the active space. These orbitals were filled with four electrons for **BD** and six electrons for **HT**.

With regard to exchange functionals in the DFT calculations, either the local spin density functional of Slater (S),[19] or the nonlocal gradient-corrected functional of Becke (B)[20] was used. Concerning the correlation functionals, the local spin density correlation functional of Vosko−Wilk−Nusair (VWN)[21] or the nonlocal gradient-corrected functionals of Lee−Yang−Parr (LYP)[22] or Perdew−Wang (PW91)[23] were used. The combined exchange−correlation functionals investigated are SVWN, SLYP, BVWN, BLYP, and BPW91. Finally, the three-parameter hybrid formula of Becke (B3) for the exchange part[24] was used with LYP and PW91 in combinations B3LYP and B3PW91. In all of these calculations the 6-31G(d,p) basis set was utilized. BLYP calculations were also done with the correlation consistent cc-pVDZ basis set of Dunning,[57] as well as with the 6-31l+G(d,p) basis set of Pople and co-workers,[61] which is of valence triple-zeta character with polarization functions and with diffuse functions added to the C atoms.

The calculations were performed with the Gaussian94 and MOLCAS4 program packages.[62,63]

Results and Discussion

The structures of 1,3-butadiene (**BD**) and 1,3,5-hexatriene (**HT**) that have been investigated are found in Scheme 2. Energy data for various conformers of the two molecules are given in Tables 1 and 3 together with information on the character of the stationary points. The corresponding geometrical parameters are found in Tables 2 and 4, and the compositions of the CASSCF wave functions for the T_1 states are given in Table 5. Finally, potential energy surfaces for twisting around the C═C bonds in the two polyenes are seen in Figures 1−3. The text is ordered so that results from electron-correlated ab initio methods appear first, and thereafter, we make comparisons with UHF and DFT. Within each section we first discuss vertical S_0−T_1 excitations and relaxed T_1 energies for the planar structures. Subsequently, the geometries that correspond to stationary points and the shapes of T_1 PESs are treated.

The first triplet excited states of polyenes can normally be described by a single reference determinant wave function.

SCHEME 2

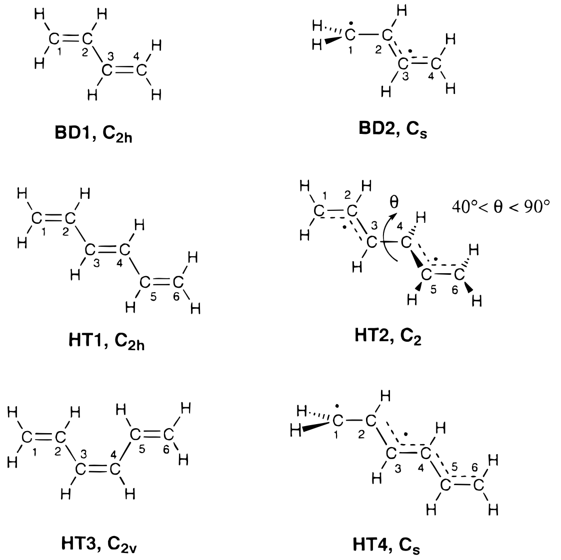

BD1, C_{2h}
BD2, C_s
HT1, C_{2h}
HT2, C_2
HT3, C_{2v}
HT4, C_s

TABLE 1: Relative T_1 Energies of 1,3-Butadiene (BD) Conformers for Rotation around Formal Double Bonds[a]

	BD1	**BD** (ZPE)	**BD2**	**BD2** (ZPE)
experiment	59.7,[b] *74.2*[c]			
CASSCF(4,4)/6-31G(d,p)	59.9, *77.5*	55.8 (0)	56.1	53.1 (0)
CASPT2/[6s3p1d/2s1p]// CASSCF(4,4)/6-31G(d,p)	56.9, *72.0*		53.5	
PUMP4(SDTQ)/cc-pVDZ// UMP2/cc-pVDZ	61.4, *77.9*		56.9	
UHF/6-31G(d,p)	39.5, *71.4*	38.5 (0)	29.3	25.3 (0)
USVWN/6-31G(d,p)	66.6, *79.0*		62.0	
USLYP/6-31G(d,p)	66.4, *78.4*		61.6	
UBVWN/6-31G(d,p)	59.4, *73.6*		56.0	
UBLYP/6-31G(d,p)	59.3, *73.0*	56.4 (0)	55.7	52.9 (0)
UBLYP/cc-pVDZ	59.1		55.7	
UBLYP/6-311+G(d,p)	59.4		55.7	
UBPW91/6-31G(d,p)	58.0, *71.8*		53.8	
UB3LYP/6-31G(d,p)	58.5, *75.4*	55.4 (0)	53.9	50.6 (0)
UB3PW91/6-31G(d,p)	57.1, *74.0*		52.1	

[a] Relative energies are given in kcal/mol with regard to the **BD**1 conformation in the S_0 state. The first entry in normal print corresponds to relaxed T_1 energies, whereas the second entry in italics corresponds to vertical T_1 energies. Columns marked with ZPE include zero-point vibrational corrections to the electronic energy. Numbers in parenthesis refer to number of imaginary frequencies. [b] Value from ref 32. [c] Value from ref 25.

However, a multireference determinant approach could be required when investigating twisting around C═C bonds where less excitation is localized, that is for bonds where *Z*/*E*-isomerization is likely to occur according to the adiabatic mechanism (Scheme 1). In the ab initio part of the study, UMP4(SDTQ), i.e., a single-reference determinant method, was utilized. However, the multireference methods CASSCF and CASPT2 were also applied at selected geometries.

1,3-Butadiene. The vertical $1^1A_g-1^3B_u$ excitation of **BD** has previously been studied computationally by several groups, and is accurately calculated by Roos et al. at CASPT2 and by Freed and Graham at VSEH levels to be 3.20 and 3.23 eV,[29-31] in excellent agreement with the experimental value of 3.22 eV (74.2 kcal/mol).[25] When the CASPT2/[6s3p1d/2s1p] calculation is performed on the optimal CASSCF(4,4)/6-31G(d,p) geometry with an active space that includes only the valence π-orbitals of **BD** a slightly larger disagreement is found since a vertical T_1 energy of 3.12 eV (72.0 kcal/mol) is obtained. A similar calculation based on the electron diffraction geometry of **BD** as determined by Haugen and Traetteberg,[64] led to an energy of 3.16 eV (73.2 kcal/mol). Thus, the small deviation of 0.04 eV from the previously calculated energy[31] is due to our restriction of the active space used for the CASSCF reference wave function. Calculation at the PUMP4(SDTQ,full)/cc-pVDZ//UMP2(full)/cc-pVDZ level yield a vertical excitation energy of 3.38 eV (77.9 kcal/mol), and at the CASSCF(4,4)/6-3lG(d,p) level it is 3.36 eV (77.5 kcal/mol).

The main purpose of this study is, however, to compute potential energy surfaces (PESs) for *Z*/*E*-isomerization of polyenes with various methods, and the 0−0 $S_0 \rightarrow T_1$ transitions are therefore important. The experimentally determined value for the relaxed T_1 energy of **BD1** is 59.7 kcal/mol[32] and, thus, in good agreement with those calculated at PUMP4(SDTQ)//UMP2, CASSCF, and CASPT2//CASSCF levels (56.9−61.4 kcal/mol; Table 1). When ZPE corrections are made to the CASSCF S_0-T_1 energy splitting of **BD1**, a value of 55.8 kcal/mol is obtained. Since the relaxed T_1 energy after ZPE corrections at the CASSCF level is lower than the experimentally determined value, it seems as if the PUMP4(SDTQ)//UMP2 result is in best accordance with experiment since this energy also should be lowered when vibrationally corrected.

The quality of the T_1 geometries calculated at UMP2/cc-pVDZ level, used subsequently for PUMP4(SDTQ)/cc-pVDZ single point energy calculations, was analyzed. Accordingly, we performed UMP4(SDQ)/cc-pVDZ geometry optimizations of **BD1** and **BD2** in the T_1 state. As seen in Table 2, the bond lengths vary in the third decimal (0.006 Å) and the deviations in the bond angles are at most 0.4° when going from UMP2 to UMP4(SDQ). Since the spin contamination of the UHF reference wave function is negligible for **BD** ($2.0 \leq \langle \hat{S}^2 \rangle \leq 2.1$), UMP2 should correctly describe triplet-state geometries for this molecule. There is also a good agreement between UMP2 and CASSCF T_1-state geometries, and we therefore keep to UMP2 geometries for PUMP4(SDTQ) energy calculations throughout this study and also for **HT** even though spin contamination is larger in this case.

The potential energy surface at the PUMP4(SDTQ)//UMP2 level for twisting around a C═C bond is seen in Figure 1. Noteworthy is that at all electron-correlated ab initio levels there is a minimum at the twisted geometry **BD2** located 3.4−4.5 kcal/mol below **BD1** (Table 1), and thereby, the energy lowering upon rotation of a methylene group is slightly exaggerated since Wilbrandt and co-workers determined the lowering to be less than 2 kcal/mol.[40] However, inclusion of the zero-point vibrational energy at the CASSCF level leads to a reduction in this difference from 3.8 to 2.7 kcal/mol, in better accordance with experiments. It should be noted that both **BD1** and **BD2** are minima at the CASSCF level.

For longer polyenes, high-quality ab initio methods will become prohibitive for computational reasons, and there is a need to find less costly methods for calculation of polyene T_1 states. As a first choice one might think of UHF. However, even though spin contamination is low for **BD** in the T_1 state, UHF/6-31G(d,p) cannot describe the PES adequately (Figure 1). The S_0-T_1 energy gap at **BD1** is approximately 20 kcal/mol smaller than at CASSCF, CASPT2, and PUMP4(SDTQ)//UMP2 levels, and the difference in relative energy between **BD1** and **BD2** is 10 kcal/mol. Clearly, UHF leads to an incorrect description of the π-bonding character of the CC bonds, indicated in, for example, the C2C3 bond length (Table 2). This fact makes the drop in T_1 energy at **BD2** exaggerated at the

TABLE 2: Geometrical Parameters of 1,3-Butadiene (BD) conformers in the T_1 State[a]

	C1−C2	C2−C3	C3−C4	C1−C2−C3	C2−C3−C4	D1[b]	D2[c]
BD1 (S_0)							
CASSCF(4,4)/6-31G(d,p)	1.344	1.465		124.1			
MP4(SDQ)/cc-pVDZ	1.350	1.472		123.8			
MP2/cc-pVDZ	1.352	1.463		123.6			
HF/6-31G(d,p)	1.322	1.467		124.1			
SVWN/6-31G(d,p)	1.340	1.438		124.0			
BLYP/6-31G(d,p)	1.352	1.461		124.5			
B3LYP/6-31G(d,p)	1.340	1.457		124.3			
BD1 (T_1)							
CASSCF(4,4)/6-31G(d,p)	1.458	1.361		124.4			
UMP4(SDQ)/cc-pVDZ	1.468	1.363		124.2			
UMP2/cc-pVDZ	1.462	1.366		124.1			
UHF/6-31G(d,p)	1.467	1.329		124.6			
USVWN/6-31G(d,p)	1.437	1.362		124.8			
UBLYP/6-31G(d,p)	1.460	1.374		125.1			
UB3LYP/6-31G(d,p)	1.454	1.358		124.9			
BD2 (T_1)							
CASSCF(4,4)/6-31G(d,p)	1.475	1.396	1.387	123.7	124.5	99.8	
UMP4(SDQ)/cc-pVDZ	1.477	1.395	1.390	124.3	124.3	95.1	
UMP2/cc-pVDZ	1.471	1.389	1.384	124.3	124.3	95.5	
UHF/6-31G(d,p)	1.476	1.393	1.390	123.8	124.4	96.7	
USVWN/6-31G(d,p)	1.436	1.391	1.374	125.7	124.5	93.3	
UBLYP/6-31G(d,p)	1.466	1.405	1.391	125.3	125.1	93.6	
UB3LYP/6-31G(d,p)	1.462	1.395	1.383	125.0	124.8	93.6	

[a] Distances in angstroms, angles in degrees. Numbering of atoms according to Scheme 2. [b] D1 stands for dihedral angle C1−C2−C3−C4. [c] D2 stands for dihedral angle H−C1−C2−C3.

TABLE 3: Relative T_1 Energies of 1,3,5-Hexatriene (HT) Conformers for Rotation around Formal Double Bonds[a]

	HT1	**HT1** (ZPE)	**HT2**	**HT2** (ZPE)	**HT3**	**HT3** (ZPE)	**HT4**	**HT4** (ZPE)
experiment	46.9,[b] *59.4−60.1*[c]				(47.7)[b]			
CASSCF(6,6)/6-31G(d,p)	48.6, *65.4*		48.3		51.0 (49.2)		52.6	
CASPT2/[6s3p1d/2s1p]//CASSCF(6,6)/6-31G(d,p)	43.9, *57.4*		43.9		46.2 (44.6)		49.5	
PUMP4(SDTQ)/cc-pVDZ//UMP2/cc-pVDZ	50.9, *66.9*		49.3		53.2 (51.6)		53.8	
UHF/6-31G(d,p)	21.8	16.9 (1)	16.6	12.5 (0)	24.0 (22.0)	19.3 (1)	21.0	16.5 (0)
USVWN/6-31G(d,p)	50.5, *59.7*		51.6		52.8 (51.3)		56.6	
USLYP/6-31G(d,p)	50.2		51.1		52.3 (51.1)		56.2	
UBVWN/6-31G(d,p)	45.1		46.9		47.8 (45.7)		51.1	
UBLYP/6-31G(d,p)	44.8, *55.4*	42.2 (0)	46.6	43.1 (0)	47.4 (45.5)	44.7 (1)	50.8	47.6 (0)
UBLYP/cc-pVDZ	44.8		46.5		47.5 (45.5)		50.9	
UBLYP/6-311+G(d,p)	45.2		46.6		47.8 (45.9)		50.9	
UBPW91/6-31G(d,p)	43.9		45.1		46.5 (44.6)		49.1	
UB3LYP/6-31G(d,p)	44.3, *58.5*		44.6		46.9 (45.0)		49.0	
UB3PW91/6-31G(d,p)	43.2		43.1		45.8 (43.9)		47.3	

[a] Relative energies are given in kcal/mol with regard to the **HT1** conformation in the S_0 state. For **HT3** T_1 energies are also given in parentheses relative to the S_0 energy of **HT3**. First entry in normal print corresponds to relaxed T_1 energies, whereas the second entry in italics corresponds to vertical T_1 energies. Columns marked with ZPE include zero-point vibrational corrections to the absolute energy. Integer value in parentheses indicate number of imaginary frequencies. [b] Value from ref 44. Given relative to the S_0 states of **HT1** and **HT3**. [c] Values from refs 44 and 66.

UHF level, so that the agreement with experimental observations is rather poor.

Nevertheless, UHF together with the STO-3G minimal basis set was recently utilized by Kikuchi and co-workers to investigate twisting around various C═C bonds in a range of polyenes.[47,48] It was suggested that the triplet state of planar polyenes in some cases must be described by multiconfigurational SCF methods due to a “resonating biradical” character. However, an investigation of the multireference character of the T_1 state of **BD** gives at hand that there is merely little such character along the twisting of the C═C bonds. In **BD1** and **BD2**, the leading configuration, which consists of the single-electron HOMO−LUMO excitation, contributes 93 and 92% at the CASSCF(4,4)/6-31G(d,p) level (Table 5). Noteworthy is that a stability analysis of the UHF/STO-3G wave function for the T_1 state reveals an internal instability, but this is presumably due to the poor overlap between the STO-3G basis functions on adjacent C atoms. The instability naturally goes away when larger basis sets are utilized, and conclusions based on UHF/STO-3G calculations should therefore be questioned.

In summary, UHF is not a suitable method either for a quantitative or a qualitative description of the T_1 PES of **BD**, and there should be three reasons for this failure of UHF. First, insufficient description of electron correlation leads to an underestimation of the absolute energy of the S_0 state, where the electron pair that occupies the HOMO (i.e., the π_2-orbital) is in more need of dynamic electron correlation than the two separated electrons in the π_2- and π_3-orbitals occupied in the T_1 state. Secondly, the tendency of HF to overestimate bonding, and accordingly, to improperly describe conjugated systems, gives formal CC single bonds too much double-bond character in the T_1 state, and vice versa for formal CC double bonds. Finally, for longer polyenes, spin contamination of the UHF wave function becomes a major problem, as will be seen for **HT**. It is therefore necessary to seek other computationally cheap methods.

TABLE 4: Geometrical Parameters of 1,3,5-Hexatriene (HT) Conformations in the T_1 State for Rotations around Formal Double Bonds[a]

	C1−C2	C2−C3	C3−C4	C4−C5	C5−C6	C1−C2−C3	C2−C3−C4	C3−C4−C5	C4−C5−C6	D1[b]	D2[c]	D3[d]
HT1 (S_0)												
CASSCF(6,6)/6-31G(d,p)	1.345	1.460	1.351			124.2	124.0					
MP2/cc-pVDZ	1.354	1.457	1.362			123.8	123.8					
HF/6-31G(d,p)	1.323	1.463	1.329			124.2	124.0					
SVWN/6-31G(d,p)	1.343	1.430	1.353			124.2	124.2					
BLYP/6-31G(d,p)	1.355	1.452	1.366			124.7	124.5					
B3LYP/6-31G(d,p)	1.343	1.449	1.352			124.5	124.3					
HT1 (T1)												
CASSCF(6,6)/6-31G(d,p)	1.414	1.375	1.471			124.7	123.9					
UMP2/cc-pVDZ	1.427	1.352	1.459			124.6	124.1					
UHF/6-31G(d,p)	1.405	1.370	1.500			124.7	123.5					
USVWN/6-31G(d,p)	1.398	1.373	1.439			125.0	124.2					
UBLYP/6-31 G(d,p)	1.416	1.387	1.465			125.4	124.4					
UB3LYP/6-31G(d,p)	1.408	1.374	1.465			125.2	124.2					
HT2 (T_1)												
CASSCF(6,6)/6-31G(d,p)	1.389	1.394	1.481			124.5	123.7			85.1	0.2	179.6
UMP2/cc-pVDZ	1.387	1.385	1.477			124.4	123.7			79.4	0.2	179.6
UHF/6-31G(d,p)	1.390	1.392	1.483			124.4	123.7			88.3	0.1	179.4
USVWN/6-31G(d,p)	1.387	1.379	1.447			124.8	124.1			42.5	0.2	175.7
UBLYP/6-31G(d,p)	1.402	1.395	1.476			125.2	124.9			52.2	0.2	177.3
UB3LYP/6-31G(d,p)	1.385	1.391	1.472			124.9	124.5			78.1	0.3	179.6
HT3 (T_1)												
CASSCF(6,6)/6-31G(d,p)	1.412	1.376	1.480			124.1	126.7					
UMP2/cc-pVDZ	1.419	1.356	1.476			124.0	126.8					
UHF/6-31 G(d,p)	1.403	1.374	1.509			124.1	126.4					
USVWN/6-31G(d,p)	1.395	1.375	1.450			124.4	126.2					
UBLYP/6-31G(d,p)	1.414	1.389	1.476			124.8	127.2					
UB3LYP/6-31G(d,p)	1.405	1.375	1.476			124.6	127.0					
HT4 (T_1)												
CASSCF(6,6)/6-31G(d,p)	1.477	1.371	1.419	1.422	1.366	124.0	124.4	123.6	124.6		100.4	
UMP2/cc-pVDZ	1.473	1.357	1.420	1.418	1.357	124.8	124.2	123.4	124.5		96.4	
UHF/6-31G(d,p)	1.477	1.375	1.415	1.414	1.374	124.0	124.2	123.7	124.4		97.1	
US9WN/6-31G(d,p)	1.439	1.371	1.398	1.404	1.360	125.9	124.3	123.8	124.8		93.8	
UBLYP/6-31G(d,p)	1.468	1.385	1.419	1.423	1.375	125.5	124.8	124.1	125.2		94.2	
UB3LYP/6-31G(d,p)	1.463	1.373	1.412	1.415	1.364	125.2	124.6	124.0	125.0		94.4	

[a] Distances in angstroms, angles in degrees. Numbering of atoms according to Scheme 2. [b] D1 stands for dihedral angle C2−C3−C4−C5. [c] D2 stands for dihedral angle H−C1−C2−C3. [d] D3 stands for dihedral angle C1−C2−C3−C4.

TABLE 5: Composition of CASSCF(*n*,*n*)/6-31G(d,p) T_1 State Wave Functions of BD and HT[a]

BD1	$(\pi_1)^2\pi_2\pi_3$ (92.7%), $\pi_1(\pi_2)^2\pi_4$ (3.2%), $\pi_2\pi_3(\pi_4)^2$ (2.0%)
BD2	$(\pi_1)^2\pi_2\pi_3$ (92.1%), $\pi_1\pi_2\bar{\pi}_3\pi_4$ (4.0%), $\pi_1\pi_2\pi_3\bar{\pi}_4$ (1.3%), $\pi_2\pi_3(\pi_4)^2$ (2.1%)
HT1	$(\pi_1)^2(\pi_2)^2\pi_3\pi_4$ (85.1%), $(\pi_1)^2\pi_2(\pi_3)^2\pi_5$ (3.0%), $(\pi_1)^2\pi_2(\pi_4)^2\pi_5$(1.0%), $\pi_1(\pi_2)^2(\pi_3)^2\pi_6$ (1.5%), $\pi_1(\pi_2)^2\pi_4\pi_5\bar{\pi}_6$ (1.1%)
HT2	$(\pi_1)^2(\pi_2)^2\pi_3\pi_4$ (84.9%), $(\pi_1)^2\pi_2\bar{\pi}_3\pi_4\pi_6$ (1.7%), $\pi_1(\pi_2)^2\bar{\pi}_3\pi_4\pi_5$ (1.8%), $\pi_1(\pi_2)^2(\pi_3)^2\pi_6$ (1.1%), $\pi_1(\pi_2)^2\pi_3\pi_4\bar{\pi}_5$ (1.2%), $(\pi_1)^2\pi_2\pi_3\pi_4\bar{\pi}_6$(1.2%), $\pi_1\bar{\pi}_2\pi_3\pi_4\pi_5\bar{\pi}_6$ (1.3%)
HT3	$(\pi_1)^2(\pi_2)^2\pi_3\pi_4$ (84.7%), $(\pi_1)^2\pi_2(\pi_3)^2\pi_5$ (3.1%), $\pi_1(\pi_2)^2\bar{\pi}_3\pi_4\pi_5$ (1.0%), $(\pi_1)^2\pi_2(\pi_4)^2\pi_5$ (1.0%), $\pi_1(\pi_2)^2(\pi_3)^2\pi_6$ (1.5%), $\pi_1\bar{\pi}_2\pi_3\pi_4\pi_5\bar{\pi}_6$ (1.1%)
HT4	$(\pi_1)^2(\pi_2)^2\pi_3\pi_4$ (86.2%), $(\pi_1)^2\pi_2\pi_3\bar{\pi}_4\pi_5$ (3.5%), $(\pi_1)^2\pi_2\pi_3\pi_4\bar{\pi}_5$ (1.1%), $\pi_1(\pi_2)^2\pi_3\bar{\pi}_4\pi_6$ (1.8%), $\pi_1\bar{\pi}_2\pi_3(\pi_4)^2\pi_5$ (1.7%), $\pi_1\bar{\pi}_2\pi_3\pi_4\pi_5\bar{\pi}_6$ (1.3%)

[a] Only configurations that contribute 1% or more are tabulated. For **BD2** the molecular orbital mainly centered on the methyl radical is π_2, whereas for **HT4** it is π_3.

Accordingly, we tested several density functional methods ranging from the LSDA method SVWN to the hybrid functional method B3PW91. At a first stage, vertical S_0-T_1 excitation energies were calculated. As seen in Table 1, USVWN/6-31G(d,p) gives a result of 3.43 eV (79.0 kcal/mol), which is higher by 0.21 eV (4.8 kcal/mol) than the experimental value of 3.22 eV (74.1 kcal/mol).[25] The energy is similar at the USLYP level, i.e. when gradient corrections are made to the correlation part of the functional. A better agreement with experiments,[25] and previous CASPT2 and VSEH calculations,[29−31] is obtained when the Becke gradient-corrected exchange functional is applied, since UBVWN/6-3lG(d,p) gives a vertical excitation energy of 3.19 eV (73.6 kcal/mol). The other DFT methods listed in Table 1 give energies within the range 3.13−3.26 eV (72−75 kcal/mol), with the best agreement obtained by UB3PW91/6-31G-(d,p).

With regard to relaxed T_1 energies, USVWN and USLYP deviate more than acceptable from electron-correlated ab initio methods (66.6 and 66.4 kcal/mol vs 56.9−61.4 kcal/mol). Once again, usage of the Becke gradient-corrected exchange in UBVWN, UBLYP, and UBPW91 leads to a considerable improvement (58.0−59.4 kcal/mol), with UBVWN/6-31G(d,p) having the best performance. Moreover, hybrid functionals such as UB3LYP and UB3PW91 lead to relaxed T_1 energies of **BD1** which are lower by 1−4 kcal/mol when compared to the corresponding pure DFT and, thereby, to similar energies as CASPT2 (Table 1). The fact that a change from the B to B3 exchange functional leads to an energy lowering could result from inclusion of Hartree−Fock exchange into the hybrid formula since UHF underestimates the T_1 energy of **BD**. Finally, a note should be given to the fact that USLYP gives a deviation in the T_1 energy whereas UBWVN agrees well with the ab initio results. Clearly, it is more important that the exchange functional than that the correlation functional is gradient corrected for a proper ΔE_{S-T} to be calculated.

The choice of basis set is normally important; this is also true in DFT calculations. Scheiner and co-workers recently

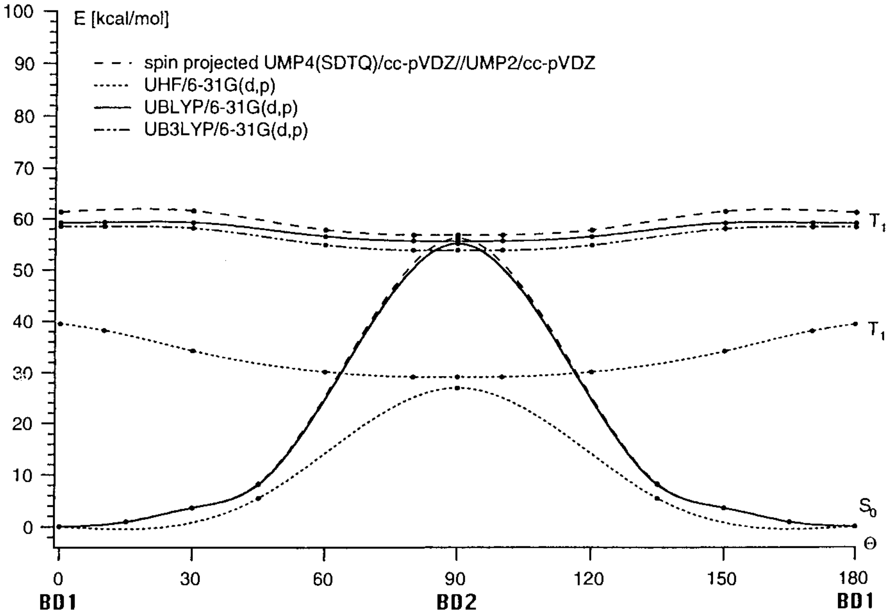

Figure 1. S_0 and T_1 potential energy surfaces for rotation of a C═C bond in **BD** at PUMP4(SDTQ)/cc-pVDZ//UMP2/cc-pVDZ, UHF/6-31G(d,p), UBLYP/6-31G(d,p), and UB3LYP/6-31G(d,p) levels. The S_0 PES at UB3LYP/6-31G(d,p) level is omitted from the figure. The angle Θ corresponds to the H1−C1−C2−C3 dihedral angle.

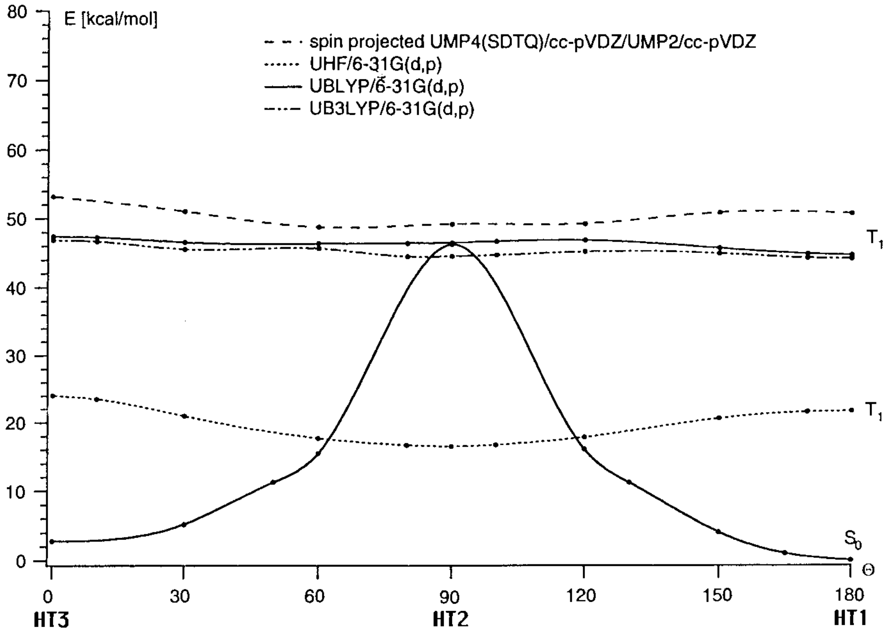

Figure 2. S_0 and T_1 potential energy surfaces for rotation of the central C═C bond in **HT** at PUMP4(SDTQ)/cc-pVDZ//UMP2/cc-pVDZ, UHF/6-31G(d,p), UBLYP/6-31G(d,p), and UB3LYP/6-31G(d,p) levels. The S_0 PES is plotted only at UBLYP/6-31G(d,p) level. The angle Θ corresponds to the C2−C3−C4−C5 dihedral angle.

showed that the cc-pVDZ basis set of Dunning[57] is recommendable for routine calculations.[65] It was also noted that for high accuracy in the computations a basis sets of at least triple-zeta quality was required. Accordingly, we tested the basis set dependence for the UBLYP functional at **BD1** and **BD2** since it can be expected that the T_1 state, as an excited state, might require a basis set which includes diffuse functions for a proper description. However, usage of the valence triple zeta basis set 6-311+G(d,p), which has diffuse functions on C atoms, did not substantially alter either geometries or energies for the T_1 state (Table 1). Moreover, usage of the correlation consistent basis set cc-pVDZ of Dunning leads to only small changes in this case. Conclusively, the 6-31G(d,p) basis set is fully sufficient for a description of the T_1 PES of **BD**.

It can be seen that the T_1-state geometries of **BD1** and **BD2** calculated at the UBLYP and UB3LYP levels are in good agreement with those calculated at the UMP4(SDQ) and CASSCF levels (Table 2). In general, the UB3LYP geometries are in slightly better agreement with UMP4(SDQ) results than those calculated at the UBLYP level. On the other side, usage of UHF or USVWN leads to geometries that are not always compatible with the higher level ab initio calculations.

The T_1 PESs for rotation around the C═C bonds at the UBLYP/6-31G(d,p) and UB3LYP/6-31G(d,p) levels are seen in Figure 1. It is noteworthy that both curves follow the PUMP4(SDTQ)//UMP2 curve closely and that no tendency for exaggeration is seen with regard to the valley at **BD2**, as was the case with UHF. The UB3LYP is in general lower than

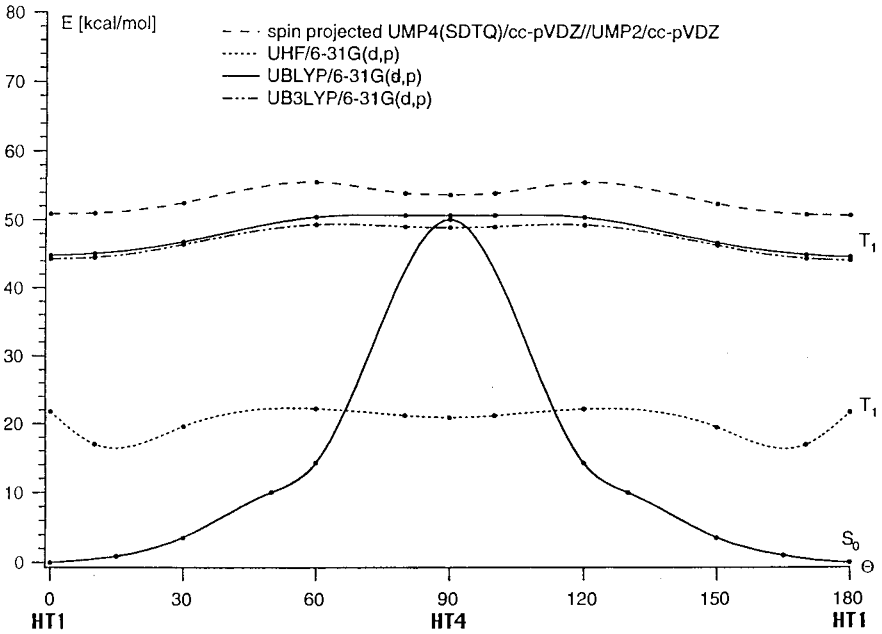

Figure 3. S_0 and T_1 Potential energy surfaces for rotation of a terminal C═C bond in **HT** at PUMP4(SDTQ)/cc-pVDZ//UMP2/cc-pVDZ, UHF/6-31G(d,p), UBLYP/6-31G(d,p) and UB3LYP/6-31G(d,p) levels. The S_0 PES is plotted only at UBLYP/6-31G(d,p) level. The angle Θ corresponds to the H1−C2−C3−C4 dihedral angle.

UBLYP by 1−2 kcal/mol, thus being 3−4 kcal/mol below PUMP4(SDTQ)//UMP2. Moreover, similar to that found at CASSCF level, the T_1 energies are lowered overall when zero-point vibrational energy corrections are made to the DFT-energies (Table 1).

Upon inclusion of ZPE corrections at the UBLYP/6-31G-(d,p) level, the difference in relative T_1 energies between **BD1** and **BD2** is merely reduced from 3.6 to 3.5 kcal/mol. The DFT methods therefore lead to results on the energy reduction for the methylene rotation that are of comparable quality to the ab initio methods used. Thus, there is still a small energy discrepancy when compared to the experiment, which revealed that the twisted structure **BD2** is not more than 2 kcal/mol lower than the planar **BD1**.[40] In general, the drop in energy when going from **BD1** to **BD2** for the hybrid functional methods is slightly larger (~5 kcal/mol) than for the nonlocal gradient-corrected methods (3−4 kcal/mol). Therefore, when compared to experimental results, it seems as if the photochemistry of **BD** in the T_1 state is better described by pure nonlocal gradient-corrected DFT methods than by hybrid functional methods.

It should finally be mentioned that spin contamination is very low in all DFT calculations along the T_1 PES of **BD**, since $\langle \hat{S}^2 \rangle$ is below 2.01 for pure DFT methods and below 2.04 for hybrid functionals.

1,3,5-Hexatriene. The vertical $1^1A_g-1^3B_u$ excitation of **HT1** is measured as 2.61 eV (60.1 kcal/mol).[66] Even though a range of high-level ab initio computations have been performed previously on the vertical $S_0 \rightarrow T_1$ excitation of **HT1**, we report here the values calculated at the CASSCF(6,6)/6-31G(d,p), CASPT2/[6s3p1d/2s1p]//CASSCF(6,6)/6-31G(d,p), and PUMP4-(SDTQ,fc)/cc-pVDZ//UMP2(full)/cc-pVDZ levels. At these levels the excitation was found in the range 2.50−2.90 eV (57.4−66.9 kcal/mol), with the best agreement for the CASPT2 calculation. Similar to **BD**, it is possible to improve the agreement for the CASPT2 energy even further to 2.52 eV by usage of the electron diffraction geometry. Use of the latter geometry for **HT1** together with a larger active space led Roos and co-workers to a vertical T_1 energy of 2.55 eV.[31] Also the VSEH method as reported by Martin and Freed (2.57 eV) give an excellent agreement with the experimental value.[30]

Central to our study are the relaxed T_1 energies of **HT1** and **HT3**, which are 48.6 and 49.2 kcal/mol at CASSCF, 43.9 and 44.6 kcal/mol at CASPT2//CASSCF, and 50.9 and 51.6 kcal/mol at PUMP4(SDTQ)//UMP2. In this regard, it should be noted that the T_1 energies are calculated relative to the corresponding S_0 states of **HT1** and **HT3**, respectively. Thus, the computed energies at CASSCF and PUMP4(SDTQ)//UMP2 levels are higher by 2−4 kcal/mol than those determined experimentally (46.9 and 47.7 kcal/mol),[44] whereas the opposite applies for CASPT2//CASSCF. It can of course be argued that similar to **BD**, the T_1 energies will be lowered when corrections for zero-point vibrational energies are included. A better agreement between experimental and calculated relaxed T_1 energies would thereby result for CASSCF and PUMP4-(SDTQ)//UMP2, whereas the deviation for CASPT2//CASSCF would increase. However, usage of a larger active space in the CASSCF calculations on which the second-order perturbation treatment in CASPT2 is based, would most likely lead to a slightly higher T_1 energy and thus to a reduction in the deviation. In addition, it should be mentioned that the uncertainty in the experimental values of the 0−0 $S_0 \rightarrow T_1$ transitions is at least 0.5 kcal/mol.[44]

The multireference character of the T_1 wave functions of **HT1** and **HT3** is low since the determinant composed of the HOMO−LUMO excitation makes up ~85% of the wave function at the CASSCF(6,6)/6-31G(d,p) level in both isomers (Table 5). This is in contradiction to what was recently stated by Kikuchi and co-workers,[47,48] who claimed that planar polyenes with odd numbers of C═C bonds must be described as "resonating biradicals" in their T_1 states and that multireference methods are needed when computing such states. It should be mentioned that Roos and co-workers recently found that *E*-stilbene in the T_1 state is described to 76% by the determinant corresponding to the HOMO−LUMO excitation.[67] It thereby seems as if single-reference determinant methods which take care of dynamic electron correlation are more appropriate for computation of the *Z*/*E*-isomerization pathways that olefins follow in their T_1 states.

Our main interest was to investigate the PES for rotation around the C=C bonds in **HT** and to see whether these surfaces are correctly described by Kohn−Sham DFT methods. Both in this and previous studies,[49] two minima on the T_1 PES could be located when the central C=C bond was rotated. These minima, which are isoenergetic at the CASSCF and CASPT2//CASSCF levels, correspond to **HT1** and **HT2**, where in the latter conformer the C2−C3−C4−C5 dihedral angle is rotated by 80−85° (Table 4). The fact that **HT1** and **HT2** are isoenergetic agrees well with findings made by Wilbrandt and co-workers from resonance Raman measurements,[41] since it was concluded that the isomers are within 1 kcal/mol in stability. At the PUMP4(SDTQ)//UMP2 level **HT2** is slightly more stable than **HT1** by 1.6 kcal/mol.

Furthermore, the T_1 energy of **HT3** compared to **HT1** is 2.3−2.4 kcal/mol higher at CASSCF, CASPT2//CASSCF, and PUMP4(SDTQ)//UMP2 levels, in minor exaggeration when compared to the experimental estimate of 0.22−2.2 kcal/mol.[41] However, it should be noted that C_{2v}-symmetric **HT3** in the T_1 state is a transition state at the UMP2(fc)/6-31G(d) level. An experimental determination of the relaxed T_1 energy of **HT3** should therefore be difficult since **HT3** will transform immediately to **HT2** when it reaches the T_1 state. As noted by Wilbrandt and co-workers,[41] the large variation in experimental values of **HT3** is most likely due to the fact that different experimental methods probe molecules with different degrees of relaxation.

Twisting around a terminal double bond of **HT** has previously been studied computationally by Malrieu and co-workers.[36] From calculations with a nonempirical Heisenberg Hamiltonian it was concluded that **HT4** is 3.6 kcal/mol above **HT1**. When computing the rotational barrier at the PUMP4(SDTQ)//UMP2, CASSCF, and CASPT2//CASSCF levels, values between 2.9 and 5.6 kcal/mol are obtained, in acceptable agreement with the previous calculation. From resonance-Raman measurements by Wilbrandt and co-workers on 1,2-divinylcyclopentene it was concluded that this rotational barrier is approximately 2 kcal/mol,[46] thus being slightly lower than all computed energy barriers.

It should be noted that the multireference character for **HT4** is low since the leading configuration contributes 86% to the T_1 wave function at CASSCF(6,6)/6-31G(d,p) level (Table 5). Therefore, since no structure on the T_1 PESs for *Z*/*E*-isomerization of **BD** and **HT** indicate the need for multireference determinant methods, the proper treatment of dynamic electron correlation is clearly of higher importance. Furthermore, the contribution from the leading configuration is constant for both molecules at all structures investigated, even though it is overall lower in **HT** than in **BD**. Also for **HT4**, which corresponds to the maximum at a pathway which should admit an adiabatic isomerization mechanism, no increased admixture of other configurations can be seen. When going from **BD2** and **HT2** to **HT4** the amount of multireference character when compared to the corresponding planar isomers does not increase. This could change slightly if the twisted structure is of much higher energy than its planar isomers. As recently noted by Kikuchi and co-workers,[68] the second most important configuration of planar **HT** is that which corresponds to the $\pi^2-\pi^5$ single excitation. However, the importance of this configuration decreases with increasing basis set and does not contribute to the wave function of **HT1** more than ~3% at the CASSCF(6,6)/6-31G(d,p) level. No other configuration makes a larger contribution than approximately 2%.

Our ab initio results are thus in accordance with previously reported experimental data for T_1 state isomerizations.[41] Rotation around the central C=C bond is more facile than rotation around either of the terminal bonds. However, this is also predicted by Hückel theory since the biradical **HT4** formed in the latter process is less stabilized by resonance than **HT2** formed in the first process. The difference in Hückel resonance stabilization energy between two allyl radicals on one hand and a pentadienyl and a methyl radical on the other is 0.192β.

As for **BD**, standard Kohn−Sham DFT methods give much better results for **HT** than UHF with regard to both energies and geometries when compared to electron-correlated ab initio results.

UHF/6-31G(d,p) gives a spin contamination in the range $2.34 \leq \langle \hat{S}^2 \rangle \leq 2.47$, and the T_1 energies are too low by roughly 30 kcal/mol (Table 3). The T_1 PESs at the UHF level also do not agree well with those calculated at the PUMP4(SDTQ)//UMP2 level (Figures 2 and 3). For example, the drop in energy by rotation of the central C=C bond is 5.2 kcal/mol, when the PES with regard to this parameter should be flat according to both more advanced calculations and experiments.[4l,45,49] Spin projection of the UHF wave function, as performed during the UMP4(SDTQ) calculation, leads to even more spurious results. In this case, the S_0-T_1 gap is for some geometries below 10 kcal/mol, whereas the correct energies are in the range 40−50 kcal/mol. Due to the very poor quality of PUHF, the curves obtained from these calculations were not plotted into Figures 2 and 3. It *is clearly not recommendable to utilize neither UHF or P-UHF when investigating T_1 states of olefins by computational means.*

When calculating **HT1** in the T_1 state at the UHF/STO-3G level, as recently done by Kikuchi and coworkers,[47,48] we obtained a spin-contaminated wave function with $\langle \hat{S}^2 \rangle = 2.6$, i.e., far from the ideal value of 2. Remarkably, there is no instability of the UHF/STO-3G T_1 wave function of **HT1**, but since it is contaminated by higher multiplets, it corresponds to a state that should be described as a partial tetraradical. Binding π-orbital overlap is less important for such a spin-contaminated species, and the fact that minimal basis sets in HF calculations of double-bonded systems lead to instabilities of the wave function is of little relevance.[69] The finding made by Kikuchi and co-workers that different T_1 energies are obtained for **HT** depending on the initial guess of the wave function, could be an effect of an insufficient basis set. Accordingly, the UHF/STO-3G results presented on T_1 states of polyenes are dubious, and the concept "resonating biradicals" could be a result of the low computational level.

Of the DFT methods, USVWN leads to a good agreement with the experimental value of the vertical T_1 energy for **HT1** (59.7 vs 60.1 kcal/mol).[32] On the other hand, methods that contain the Slater local spin-density functional for exchange give relaxed T_1 energies which in general are too high. When the Becke nonlocal gradient-corrected exchange functional is used in UBLYP and UBPW91, the vertical excitation energies are somewhat low, even though the latter methods are in good accordance with experimental values for relaxed T_1 energies. However, when ZPE corrections are added to the singlet−triplet splitting of **HT1** at the UBLYP/6-3lG(d,p) level, a value of 42.2 kcal/mol is obtained. In general, gradient-corrected DFT methods underestimate the relaxed T_1 energies of **HT** by approximately 4 kcal/mol when compared to measured values. For olefins larger than **HT** it seems as if this underestimation converges to approximately 6 kcal/mol below the experimentally determined T_1 energies.[70] Hybrid functionals such as UB3LYP give similar or just slightly lower energies than those obtained by pure gradient-corrected DFT methods, probably a result of the HF exchange as discussed in the section on **BD**. Nevertheless, both of the latter type of DFT methods clearly give acceptable energies which are bracketed by the PUMP4(SDTQ)//UMP2 and CASPT2//CASSCF calculations.

Usage of larger basis sets for the various T_1 conformers of **HT** revealed, as for **BD**, that there is no need for either diffuse or correlation consistent basis functions in UBLYP calculations (Table 3). The 6-31G(d,p) basis set is sufficient, and this should open up the possibility to compute larger olefinic systems since the combination of cheap DFT methods and a standard valence double-zeta basis set can be utilized.

It should be noted that the C_{2v}-symmetric **HT3** is also not a stable structure at UBLYP level since it corresponds to the transition state for degenerate isomerization between two forms of **HT2**. The T_1 energy differences between **HT1** and **HT3** are in the range 2.1−2.6 kcal/mol at the DFT levels and, thus, in agreement with high-level ab initio calculations and with the experimental determination (0.2−2.2 kcal/mol).[41] Furthermore, at all DFT levels the energy difference between **HT1** and **HT2** in the T_1 state is less than 1.8 kcal/mol, with **HT2** being equal or higher in energy than **HT1**. It can be noted that hybrid functional methods are in accordance with CASPT2//CASSCF and the experimental finding that the two isomers are isoenergetic, whereas nonlocal gradient-corrected DFT methods place **HT2** at a higher energy, thus in slight disagreement with our electron-correlated ab initio calculations as well as with experiments.

For all DFT methods analyzed the barrier of rotation around a terminal C═C bond is slightly exaggerated by 2−4 kcal/mol when compared to experiments performed on **DVCP,** which revealed that the barrier is 2 kcal/mol.[46] Thus, these methods give results similar to the CASPT2//CASSCF result of 5.6 kcal/mol, and zero-point vibrational energy corrections do not seem to have a large impact on this rotational barrier since the energy difference between **HT1** and **HT4** is only decreased from 6.0 to 5.4 kcal/mol at the UBLYP/6-31G(d,p) level. However, the experimental value could as mentioned in the Introduction also correspond to the energy needed to distort the central C═C bond so that a geometry is reached where spin−orbit coupling between the T_1 and S_0 states is sizable and intersystem crossing occurs. We therefore find that the energies calculated with DFT should rather be compared with the ab initio data (2.9−5.6 kcal/mol). A general observation is that the hybrid functionals give a slightly lower energy barrier than the pure gradient-corrected DFT methods and, thereby, agree more with experiments.

The T_1 PES for rotation of the central C═C bond in **HT** is sufficiently well described at the UBLYP/6-31G(d,p) and UB3LYP/6-31G(d,p) levels when compared to PUMP4(SDTQ)//UMP2 (Figure 2). Also the agreement in the T_1 PESs for terminal C═C bond rotation is acceptable as seen in Figure 3, even though the minimum at **HT4** is deeper at the PUMP4(SDTQ)//UMP2 level than at the UBLYP and UB3LYP levels. The PESs calculated with DFT should therefore be of similar quality as those obtained from electron-correlated methods such as PUMP4(SDTQ)//UMP2 and CASPT2//CASSCF. As can be concluded from relative energies of the various T_1 isomers of **HT**, the overall shape of the triplet surface might indeed be best described by hybrid functional methods, whereas the relaxed T_1 energies for planar structures are best described by pure nonlocal gradient-corrected DFT. When compared to UHF, it becomes clear that DFT calculations lead to a drastic improvement in the description of the T_1 PESs both quantitatively and qualitatively. The spurious drop in energy for the UHF curve at ∼20° for terminal C═C bond rotation has disappeared. In this regard, it should be mentioned that at no point along the T_1 PESs of **HT** was a value of $\langle \hat{S}^2 \rangle$ higher than 2.07 calculated for neither of the DFT methods, which is much smaller than found for UHF.

Finally, with regard to computed geometries there is a larger deviation between USVWN and the two ab initio methods CASSCF and UMP2 than for UBLYP and UB3LYP (Table 4). However, the ab initio values for the C2C3C4C5 dihedral angle for **HT2** are not as well reproduced by UBLYP as by UB3LYP (Table 4). There is a large variation in this angle (42−85°), with USVWN and UBLYP leading to the largest deviations when compared to CASSCF and UMP2 (79−85°). However, except for this discrepancy the UBLYP and UB3LYP geometries agree and deviations from ab initio results are minor. Interestingly, when a UMP4(SDTQ,fc)/cc-pVDZ calculation is performed at the optimal UBLYP/cc-pVDZ geometry of **HT1**, a relaxed T_1 energy which is lower by 0.6 kcal/mol is obtained as compared to when the calculation is performed at the optimal UMP2(full)/cc-pVDZ geometry. This should indicate that UBLYP gives a geometry for the T_1 state that is closer than UMP2 to the optimal UMP4(SDTQ) geometry. Noteworthy is that the C2C3 bond in T_1 excited **HT1** and **HT3** is shorter by 0.02−0.03 Å at the UMP2 level than at all other computational levels (Table 4), and it is likely that UMP2 is not the best choice for calculation of T_1 geometries of larger olefins. Since spin contamination of the UHF reference wave function increases the larger the olefin becomes, the UMP2 calculation will be deteriorated. It is therefore probable that UBLYP geometries are of higher quality than UMP2 geometries for larger polyenes, where spin contamination of UHF is sizable.

Conclusions

Among less CPU-costly methods analyzed for computations of T_1 PESs of olefins, it has been clarified that neither UHF nor spin-projected UHF are suitable methods. Quantitative as well as qualitative agreement between UHF and higher level ab initio calculations is poor. Several factors are responsible for this finding. Most obvious is spin contamination of the calculated T_1 energy, which increases the longer the polyene becomes. Moreover, the tendency of Hartree−Fock to exaggerate bonding gives formal CC double bonds too much single-bond character upon excitation of the olefin to the T_1 state. This leads to T_1 PESs that are not in accordance with those obtained from more sophisticated ab initio calculations. Finally, it is argued that insufficient description of electron correlation in HF leads to an underestimation of the singlet−triplet energy gap in olefins.

Methods that include only LSDA for exchange give energies that in most cases are too high. However, pure nonlocal gradient-corrected DFT and hybrid functional methods can correctly describe the PESs for T_1 state *Z*/*E*-photoisomerizations of olefins. The curves calculated at the UBLYP and UB3LYP levels for **BD** and **HT** are in accordance with those at the PUMP4(SDTQ)//UMP2 level. Since T_1 energies from these two types of methods are bracketed by those from CASPT2//CASSCF and PUMP4(SDTQ)//UMP2, it is concluded that results are of comparable quality as those from electron-correlated ab initio methods. Usage of hybrid functionals leads to T_1 energies that are lower than nonlocal gradient-corrected DFT by 1−2 kcal/mol, and this is most likely due to the HF exchange which is included in such functionals.

The calculated DFT data are also in good agreement with experimental findings, and the postulated isomerization mechanisms for **BD** and **HT** in T_1 states are confirmed by our DFT computations. Investigations of larger olefins could therefore be carried out with DFT methods. Hybrid functionals stabilize twisted structures as compared to planar isomeric structures by 1−2 kcal/mol more than the corresponding pure gradient-corrected DFT methods. For **HT** this leads to a better agreement for hybrid functionals with regard to the experimentally determined shape of the T_1 PESs. However, the relaxed T_1 energies for planar structures are slightly lower than found experimentally, and a better accordance for these energies is instead obtained by nonlocal gradient-corrected methods.

Moreover, triple-zeta basis sets that contain diffuse functions or correlation-consistent basis sets are not required in the computation of T_1 states of polyenes with DFT methods. The standard 6-31G(d,p) valence double-zeta basis set with polarization functions can be applied.

Geometries calculated with LSDA are not always compatible with those obtained by high-level ab initio calculations. On the other hand, geometries calculated for both **BD** and **HT** at the UBLYP and UB3LYP levels are in good agreement with those obtained at the UMP4(SDQ), CASSCF, and UMP2 levels.

Finally, spin contamination of the T_1 states of **BD** and **HT** is low in all DFT calculations. For pure DFT methods $\langle \hat{S}^2 \rangle$ is below 2.03 in all cases, whereas for hybrid functionals it is below 2.07. It should be noted that the spin contamination of **HT** at the UHF level is considerably higher.

Acknowledgment. Dr. Lars Olsson and Prof. Dieter Cremer are thanked for fruitful discussions on the applicability of DFT methods, and Prof. Olof Wennerström and Dr. Mikael Sundahl for discussions on photochemistry. Calculations were performed on the CRAY C90 computer of Nationellt Superdatorcentrum (NSC) in Linköping, Sweden. The authors acknowledge NSC for a generous allotment of computer time. Financial support from the Swedish Council for Engineering Sciences (TFR) and the Swedish Natural Science Research Council (NFR) is gratefully acknowledged.

Supporting Information Available: Tables of absolute energies for stationary points at all levels investigated, tables of vibrational frequencies at those levels indicated in Tables 1 and 3, and Cartesian coordinates resulting from the UBLYP, UB3LYP, CASSCF, and UMP2 calculations (17 pages). Ordering information is given on any current masthead page.

References and Notes

(1) (a) Rando, R. A. *Angew. Chem. Int. Ed. Engl.* **1990**, *29*, 461 (b) Sanders, G. M.; Pot, J.; Havinga, E. *Fortschr. Chem. Org. Naturst.* **1969**, *27*, 129.

(2) (a) Saltiel, J.; Sun, Y.-P. In *Photochromism: Molecules and Systems*; Dörr, H., Bouas-Laurent, H., Eds.; Elsevier: Amsterdam, 1990; p 64.

(3) Tokumaru, K.; Arai, T. *Bull. Chem. Soc. Jpn.* **1995**, *68*, 1065 and references therein.

(4) (a) Parr, R. B.; Yang, W. In *Density Functional Theory of Atoms and Molecules*; Clarendon Press, Oxford, 1989 (b) Bartolotti, L. J.; Flurchick, K. In *Reviews in Computational Chemistry*; Lipkowits, K. B., Boyd, D. B., Eds.; Vol. 7, 1996; p 187.

(5) Cramer, C. J.; Dulles, F. J.; Falvey, D. *J. Am. Chem. Soc.* **1994**, *116*, 9787.

(6) Cramer, C. J.; Dulles, F. J.; Storer, J. W.; Worthington, S. E. *Chem. Phys. Lett.* **1994**, *218*, 387.

(7) Cramer, C. J.; Dulles, F. J.; Giesen, D. J.; Almlöf, J. *Chem. Phys. Lett.* **1995**, *245*, 165.

(8) Cramer, C. J.; Smith, B. A. *J. Phys. Chem.* **1996**, *100*, 9664.

(9) Cramer, C. J.; Worthington, S. E. *J. Phys. Chem.* **1995**, *99*, 1462.

(10) Cramer, C. J.; Falvay, D. E. *Tetrahedron Lett.* **1997**, *38*, 1515.

(11) Bérces, A.; Zgierski, M. Z. *Chem. Phys. Lett.* **1996**, *257*, 61.

(12) Gunnarsson, O.; Lundquist, B. I. *Phys. Rev. B* **1976**, *13*, 4274.

(13) van Barth, U. *Phys. Rev. A* **1979**, *20*, 1693.

(14) Baker, J.; Scheiner, A.; Andzelm, J. *Chem. Phys. Lett.* **1993**, *216*, 380.

(15) Pople, J. A.; Gill, P. M. W.; Handy, N. C. *Int. J. Quantum Chem.* **1995**, *56*, 303.

(16) Wittbrodt, J. M.; Schlegel, H. B. *J. Chem. Phys.* **1996**, *105*, 6574.

(17) Goldstein, E.; Beno, B.; Houk, K. N. *J. Am. Chem. Soc.* **1996**, *118*, 6036.

(18) Edgecombe, K. E.; Becke, A. D. *Chem. Phys. Lett.* **1995**, *244*, 427.

(19) (a) Slater, J. S. *Phys. Rev.* **1951**, *81*, 385. (b) Slater, J.S. *The-Self-Consistent Field for Molecules and Solids: Quantum Theory of Molecules and Solids;* McGraw-Hill: New York, 1974; Vol. 4.

(20) Becke, A. D. *Phys. Rev. A* **1988**, *38*, 3098.

(21) Vosko, S. H.; Wilk, L.; Nusair, M. *Can. J. Phys.* **1980**, *58*, 1200.

(22) Lee, C.; Yang, W.; Parr, R. G. *Phys. Rev. B* **1988**, *37*, 785.

(23) Perdew, J. P.; Wang, Y. *Phys. Rev. B* **1992**, *45*, 13244.

(24) Becke, A. D. *J. Chem. Phys.* **1993**, *98*, 5648.

(25) Evans, D. F. *J. Chem. Soc.* **1960**, 1735.

(26) (a) Nascimento, M. A.; Goddard, W. A., III *Chem. Phys.* **1980**, *53*, 251. (b) Nascimento, M. A.; Goddard, W. A., III *Chem. Phys.* **1979**, *36*, 147.

(27) Malrieu, J. P.; Nebot-Gil, I.; Sanchez-Marin, J. *Pure Appl. Chem.* **1984**, *56*, 1241.

(28) Kitao, O.; Nakatsuji, H. *Chem. Phys. Lett.* **1988**, *143*, 528.

(29) Serrano-Andres, L.; Sanchez-Marin, J.; Nebot-Gil, I. *J. Chem. Phys.* **1992**, *97*, 7499.

(30) Graham, R. L.; Freed, K. F. *J. Chem. Phys.* **1992**, *96*, 1304.

(31) Serrano-Andres, L.; Merchan, M.; Negot-Gil, I.; Lindh, R.; Roos, B. O. *J. Chem. Phys.* **1993**, *98*, 3151.

(32) Kellogg, R. E.; Simpson, W. T. *J. Am. Chem. Soc.* **1965**, *87*, 4230.

(33) Bonacic-Koutecky, V.; Ishimaru, S. *J. Am. Chem. Soc.* **1977**, *99*, 8134.

(34) Ohmine, I.; Morokuma, K. *J. Chem. Phys.* **1980**, *73*, 1907.

(35) Bonacic-Koutecky, V.; Persico, M.; Döhnert, D. Sevin, A. *J. Am. Chem. Soc.* **1982**, *104*, 6900.

(36) Said, M.; Maynau, D.; Malrieu, J.-P. *J. Am. Chem. Soc.* **1984**, *106*, 580.

(37) Aoyagi, M.; Osamura, Y.; Iwata, S. *J. Chem. Phys.* **1985**, *83*, 1140.

(38) Minaev, B. F.; Jonsson, D.; Norman, P.; Ågren, H. *Chem. Phys.* **1995**, *194*, 19.

(39) Baird, N. C.; West, R. M. *J. Am. Chem. Soc.* **1971**, *93*, 4427.

(40) Negri, F.; Orlandi, G.; Langkilde, F. W.; Wilbrandt, R. *J. Chem. Phys.* **1990**, *92*, 4907.

(41) Langkilde, F.; Wilbrandt, R.; Møller, S.; Negri, F.; Orlandi, G. *J. Phys. Chem.* **1991**, *95*, 6884.

(42) Langkilde, F.; Wilbrandt, R.; Brouwer, A. M.; Jacobs, H. J. C.; Negri, F.; Orlandi, G. *J. Phys. Chem.* **1992**, *96*, 64.

(43) Wilbrandt, R.; Langkilde, F. W.; Brouwer, A. M.; Negri, F.; Orlandi, G. *J. Mol. Struct.* **1990**, *217*, 151.

(44) Minnaard, N. G.; Havinga, E. *Recl. Trav. Chim. Pays-Bas* **1973**, *92*, 1179.

(45) Negri, F.; Orlandi, G.; Brouwer, A. M.; Langkilde, F.; Møller, S.; Wilbrandt, R. *J. Phys. Chem.* **1991**, *95*, 6895.

(46) ten Wolde, A.; Jacobs, H. J. C.; Langkilde, F. W.; Bajdor, K.; Wilbrandt, R.; Negri, F.; Zerbretto, F.; Orlandi, G. *J. Phys. Chem.* **1994**, *98*, 9437.

(47) Takahashi, O.; Watanabe, M.; Kikuchi, O. *J. Mol. Struct. (THEOCHEM)* **1996**, *369*, 67.

(48) Takahashi, O.; Watanabe, M.; Kikuchi, O. *Tetrahedron Lett.* **1995**, *36*, 1473.

(49) Negri, F.; Orlandi, G.; Zerbretto, F.; Palmieri, P.; Tarroni, R. *Chem. Phys.* **1993**, *178*, 133.

(50) Gilbert, A.; Baggott, J. *Essential of Molecular Photochemistry*; Blackwell Scientific Publications: Oxford, 1991.

(51) Dauben, W. G.; McInnis, E. L.; Mincho, D. M. In *Rearrangements in Ground and Excited States*; De Mayo, P., Ed.; Academic Press: London, 1980; Vol. 3, pp 91−129.

(52) (a) Bernardi, F.; Olivucci, M.; Robb, M. A. *Chem. Soc. Rev.* **1996**, 321. (b) Klessinger, M. *Angew. Chem., Int. Ed. Engl.* **1995**, *34*, 549.

(53) Olivucci, M.; Ragazos, I. N.; Bernardi, F.; Robb, M. A. *J. Am. Chem. Soc.* **1993**, *115*, 3710.

(54) Olivucci, M.; Bernardi, F.; Celani, P.; Ragazos, I.; Robb, M. A. *J. Am. Chem. Soc.* **1994**, *116*, 1077.

(55) Binkley, J. S.; Pople, J. A.; Hehre, W. J. *J. Am. Chem. Soc.* **1980**, *102*, 939.

(56) Hariharan, P. S.; Pople, J. A. *Theor. Chim. Acta* **1973**, *28*, 213.

(57) (a) Dunning, T. H., Jr. *J. Chem. Phys.* **1989**, *90*, 1007. (b) Woon, D. E.; Dunning, T. H. *J. Chem. Phys.* **1993**, *98*, 1358.

(58) Sosa, C.; Schlegel, B. *Int. J. Quantum Chem.* **1986**, *24*, 1001.

(59) (a) Andersson, K.; Malmquist, P.-Å.; Roos, B. O.; Sadlej, A. J.; Wolinski, K. *J. Chem. Phys.* **1990**, *94*, 5483. (b) Andersson, K.; Malmquist, P.-Å.; Roos, B. O. *J. Phys. Chem.* **1992**, *96*, 1218.

(60) Widmark, P.-O.; Malmquist, P.-Å.; Roos, B. O. *Theor. Chim. Acta* **1990**, *77*, 291.

(61) Krishnan, R.; Binkley, J. S.; Seeger, R.; Pople, J. A. *J. Chem. Phys.* **1980**, *72*, 650.

(62) Frisch, M. J.; Trucks, G. W; Schlegel, H. B.; Gill, P. W. M.; Johnson, B. G.; Robb, M. A.; Cheeseman, J. R.; Keith, T.; Petersson, G. A.; Montgomery, J. A.; Raghavachari, K.; Al-Laham, M. A.; Zakrzewski, V. G.; Ortiz, J. V.; Foresman, J. B.; Cioslowski, J.; Stefanov, B. B.; Nanayakkara, A.; Challacombe, M.; Peng, C. Y.; Ayala, P. Y.; Chen, W.; Wong, M. W.; Andres, J. L.; Repogle, R. S.; Gomperts, R.; Martin, R. L.; Fox, D. J.; Binkley, J. S.; Defrees, D. J.; Baker, J.; Stewart, J. P., Head-Gordon, M.; Gonzales, C.; Pople, J. A. *Gaussian 94*, Revision C.3; Gaussian Inc.: Pittsburgh, PA, 1995.

(63) Andersson, K.; Blomberg, M. R. A.; Fülscher, M. P.; Karlström, G.; Lindh, R., Malmquist, P.-Å.; Neogrady, P.; Olson, J.; Roos, B. O.; Sadlej, A. J.; Schutz, M.; Seijo, L.; Siegbahn, P. E. M.; Widmark, P.-O. *MOLCAS4*; Lund, Sweden, 1997.

(64) Haugen, W.; Traetteberg, M. *Acta Chem. Scand.* **1966**, *20*, 1726.

(65) Schreiner, A. C.; Baker, J.; Andzelm, J. W. *J. Comput. Chem.* **1997**, *18*, 775.

(66) Flicker, W. M.; Mosher, O. A.; Kuppermann, A. *Chem. Phys. Lett.* **1977**, *45*, 492.

(67) Molina, V.; Merchan, M.; Roos, B. O. *J. Phys. Chem.* **1997**, *101*, 3478.

(68) Takahashi, O.; Watanabe, M.; Kikuchi, O. *Int. J. Quantum Chem.* **1998**, *67*, 101.

(69) Chambaud, G.; Levy, B.; Millie, P. *Theoret. Chim. Acta* **1978**, *48*, 103.

(70) Brink, M.; Jonson, H.; Ottosson, C.-H. Manuscript in preparation.